Author Manuscript

Author Manuscript

Author Manuscript

Author Manuscript

HHS Public Access

Author manuscript

Environ Sci Technol. Author manuscript; available in PMC 2019 May 15.

Published in final edited form as:

Environ Sci Technol. 2018 May 15; 52(10): 6000–6008. doi:10.1021/acs.est.8b00612.

HUMAN LIVER MICROSOMES ATROPSELECTIVELY METABOLIZE 2,2′,3,4′,6-PENTACHLOROBIPHENYL (PCB 91) TO A 1,2-SHIFT PRODUCT AS THE MAJOR METABOLITE

Eric Uwimana, **Xueshu Li**, and **Hans-Joachim Lehmler***

Department of Occupational and Environmental Health, The University of Iowa, Iowa City, IA

Abstract

Polychlorinated biphenlys (PCBs) and their hydroxylated metabolites (OH-PCBs) have been implicated in neurodevelopmental disorders. Several neurotoxic PCBs, such as PCB 91, are chiral because they form stable rotational isomers, or atropisomers, that are non-superimposable mirror images of each other. Because only limited information about the metabolism of these PCBs by human cytochrome P450 (P450) enzymes is available, we investigated the biotransformation of PCB 91 to OH-PCBs by human liver microsomes (HLMs). Racemic PCB 91 was incubated with pooled or individual donor HLMs at 37 °C, and levels and chiral signatures of PCB 91 and its metabolites were determined. Several OH-PCBs were formed in the order 2,2′,4,4′,6-pentachlorobiphenyl-3-ol (3-100; 1,2 shift product) > 2,2′,3,4′,6-pentachlorobiphenyl-5-ol (5-91) >> 2,2′,3,4′,6-pentachlorobiphenyl-4-ol (4-91) >> 4,5-dihydroxy-2,2′,3,4′,6-pentachlorobiphenyl (4,5-91). Metabolite formation rates displayed inter-individual variability. The first eluting atropisomers of PCB 91, 3-100 and 4-91, and the second eluting atropisomer of 5-91 were enriched in most metabolism studies. The unexpected, preferential formation of a 1,2-shift product and the variability of the OH-PCBs profiles in experiments with individual donor HLMs underline the need for further systematic studies of the atropselective metabolism of PCBs in humans.

TOC image

Corresponding Author: Dr. Hans-Joachim Lehmler, The University of Iowa, Department of Occupational and Environmental Health, University of Iowa Research Park, #164 MTF, Iowa City, IA 52242-5000, Phone: (319) 335-4310, Fax: (319) 335-4290, hans-ioachim-lehmler@uiowa.edu.

Supporting Information

Authentication of PCB 91, including representative gas chromatogram and mass spectrum of PCB 91; levels and formation rates of OH-PCB metabolites; enantiomeric fractions of PCB 91 and its hydroxylated metabolites; and mass spectra of the methylated derivatives of OH-PCBs. This material is available free of charge via the Internet at http://pubs.acs.org.

Conflict of Interest Statement

The authors declare no competing financial interest.

Author Manuscript Author Manuscript Author Manuscript Author Manuscript

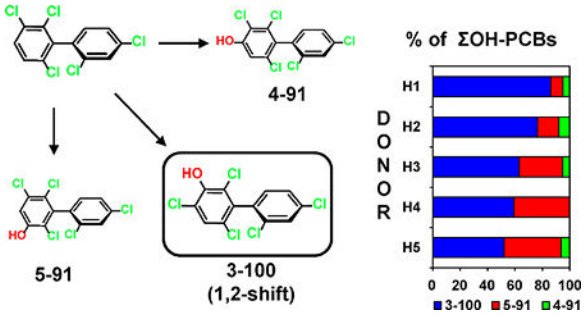

Introduction

Exposure to polychlorinated biphenyls (PCBs) has been associated with a range of adverse health outcomes, including cancer, neurological, reproductive, endocrine, and other non-cancer effects.[1] PCB congeners with multiple *ortho* chlorines are important components of technical PCB mixtures and have been detected in the environment, wildlife and humans.[2, 3] Nineteen *ortho* substituted PCB congeners, for example PCB 91, PCB 95 and PCB 136 (2,2′,3,3′,6,6′-hexachlorobiphenyl), display axial chirality and exist as rotational isomers, or atropisomers, that are non-superimposable mirror images of each other.[3, 4] Exposure of laboratory animals and humans to these chiral PCB congeners has been linked to neurodevelopmental disorders,[5, 6] possibly by mechanisms involving PCB-mediated disruption of the calcium homeostasis in the developing brain.[7–10]

Evidence suggests that chiral PCBs undergo enantiomeric enrichment in the environment and atropselectively affect the activity of drug metabolizing enzymes and endpoints implicated in PCB-mediated neurotoxicity.[2–4] Chiral PCBs undergo atropisomeric enrichment in aquatic and terrestrial food chains, thus making the biotic environment a potential source of human exposure to non-racemic chiral PCB residues.[3,11] For example, several studies have reported an enrichment of the PCB 91 atropisomer eluting second on the Chirasil-Dex (CD) column (E_2-PCB 91) in certain fish species.[12, 13] In contrast, limited human biomonitoring data revealed an enrichment of the PCB 91 atropisomer eluting first on the CD column (E_1-PCB 91) in human breast milk from Spain.[14] Thus, humans could be exposed via the diet to non-racemic chiral signatures of chiral PCBs, such as PCB 91. Alternatively, chiral PCBs may undergo atropselective metabolism to hydroxylated PCBs (OH-PCBs)[15, 16] *in vivo* following exposure to racemic PCB residues in the diet or by inhalation.

In addition to the parent PCBs, OH-PCBs are emerging as environmentally relevant contaminants which display toxicity towards wildlife and humans.[17, 18] They have been detected in wildlife, laboratory animals and humans and can reach levels comparable to levels of the parent compound *in vivo*.[17–21] Like the parent PCBs, OH-PCBs represent a human health concern because they cross the placenta,[22] accumulate in target fetal tissues,[23] and are present in the developing rat brain.[19] OH-PCBs have been linked to adverse health outcomes in laboratory and epidemiological studies, such as endocrine disruptions and cardiovascular effects.[18] OH-PCBs may also be developmental neurotoxicants, possibly by mechanism involving altered calcium homeostasis.[7] Importantly, epidemiological studies

Author Manuscript Author Manuscript Author Manuscript Author Manuscript

revealed an association between OH-PCB levels and lower mental and psychomotor development in children.[24–26]

OH-PCBs derived from chiral PCB congeners[19, 27–29] are also chiral and potentially neurotoxic; however, the toxicity of pure OH-PCBs atropisomers has not been investigated to date. Chiral OH-PCBs can be formed from the parent PCBs by mammalian P450 enzymes *via* a reactive PCB arene oxide intermediate that subsequently can rearrange to OH-PCBs[30, 31] or by direct insertion of an oxygen atom into aromatic C–H bonds.[32] While structure-metabolism relationships for PCBs, in particular PCBs with multiple *ortho* substituents, have been established in rodent models,[4, 18, 33] very limited information about the metabolism of PCBs by human P450 enzymes is available.[15, 16, 34, 35] Interestingly, the chiral OH-PCB metabolite profiles and stereoselectivity (*i.e.* chiral signatures) observed in metabolism studies with HLMs can differ drastically from those reported in studies with rat or mouse enzymes.[3, 4]

To date, only the atropselective metabolism of PCB 95 and PCB 136, chiral PCBs without *para* chlorine substituents, has been investigated using HLMs.[15, 16] Because the chlorine substitution pattern influences the regioselectivity and stereoselectivity of the oxidation of individual PCB congeners, we investigated the metabolism of PCB 91 by different HLM preparations. This *para* chlorinated PCB congener is environmentally relevant[2, 36] and displays non-racemic chiral signatures in wildlife[2, 3, 11] and humans.[14] The objective of this study was to characterize the atropselective formation of OH-PCB metabolites of PCB 91 in incubations with human liver microsomes. Our results demonstrate that PCB 91 is atropselectively metabolized by human P450 enzymes to OH-PCBs by mechanisms that, at least in part, involve arene oxide intermediates. The resulting OH-PCB metabolite profiles and chiral signatures differ from those observed in metabolism studies with other chiral PCBs, such as the structurally related PCB 95, and, thus, underline the need for further studies of the metabolism of PCBs in humans and the effects of the resulting metabolites on the developing brain.

Experimental Section

Materials

PCB 91 (white solid, purity 99.9 %; see Table S1 and Figures S1–S2 for additional information), 3-methoxy-2,2′,4,4′,6-pentachlorobiphenyl (methylated derivative of 3-100), 2,2′,3,4′,6-pentachlorobiphenyl-4-ol (4-91), 2,2′,3,4′,6-pentachlorobiphenyl-5-ol (5-91) and 4,5-dimethoxy-2,2′,3,4′,6-pentachlorobiphenyl (dimethylated derivative of 4,5-91) were synthesized as previously described.[37, 38] The chemical structures and the abbreviations of the OH-PCB metabolites are shown in Figure 1. 2,2′,4,6′-Tetrachlorobiphenyl (PCB 51; internal standard for gas chromatography/time-of-flight mass spectrometry analyses [GC/TOF-MS]); 2,3,4′,5,6-pentachlorobiphenyl (PCB 117; recovery standard), 2,2′,3,4,4′,5,6,6′-octachlorobiphenyl (PCB 204; internal standard) and 2,3,3′,4,5,5′-hexachlorobiphenyl-4′-ol (4′-159; recovery standard) were purchased from AccuStandard (New Haven, CT, USA). Solutions of diazomethane in diethyl ether for the derivatization of hydroxylated PCB metabolites to methoxylated PCB derivatives were synthesized from *N*-

Author Manuscript Author Manuscript Author Manuscript Author Manuscript

methyl-*N*-nitroso-*p*-toluenesulfonamide (Diazald) using an Aldrich mini Diazald apparatus (Milwaukee, WI, USA).

β-Nicotinamide adenine dinucleotide 2′-phosphate reduced tetrasodium salt hydrate (NADPH) was purchased from Sigma-Aldrich (Milwaukee, WI, USA). Dimethyl sulfoxide (DMSO), sodium phosphate dibasic, sodium phosphate monobasic, magnesium chloride, tetrabutylammonium sulfite, sodium sulfite, and pesticide grade solvents were obtained from Fisher Scientific (Pittsburgh, PA, USA). Ultrapure water (18 mΩ) was used to prepare all aqueous solutions. The human liver microsomes used in this study include pool human liver microsomes (pool of 50, mixed gender; pHLM) and female single-donor HLMs (donors H1 to H5, age range 20-58) provided by Xenotech (Lenexa, KS, USA). Details regarding the microsomal preparations used in this study have been published previously.[15]

PCB biotransformation assays

An incubation system containing phosphate buffer (0.1 M, pH 7.4), magnesium chloride (3 mM), human liver microsomes (0.1 mg/mL), and NADPH (1 mM) was pre-incubated for 5 min at 37°C in a shaking water bath as described.[15] PCB 91 (50 μM in DMSO; ≤ 0.5% of the incubation volume)[15, 34, 39] was added to start the reaction and the mixtures were incubated for 5 or 15 min at 37 °C. The reaction was stopped by adding ice-cold sodium hydroxide (2 mL, 0.5 M) to each sample. The incubation mixture was heated at 110 °C for 10 min and each sample was extracted as described below. All incubations with PCB 91 were performed in triplicate. Blank samples containing only phosphate buffer were extracted in parallel. In addition, control incubations without PCB (DMSO only), NADPH or microsomes, and incubations with heat inactivated microsomes accompanied all microsomal experiments.[15, 33, 40, 41] No metabolites were detected in any control sample. The formation of OH-PCBs was linear for incubation times up to 15 min for individual donor HLMs or 30 min for pHLMs. Typically, ≤ 2% of the PCB 91 added to the incubation was converted to OH-PCB metabolites (Table S2).

Extraction of PCBs and metabolites

PCB 91 and its hydroxylated metabolites were simultaneously extracted from the incubation mixture following a published procedure.[15, 33, 40, 41] Briefly, samples were spiked with surrogate recovery standards PCB 117 (200 ng) and 4′-159 (68.5 ng). Hydrochloric acid (6 M, 1 mL) was added, followed by 2-propanol (5 mL). The samples were extracted with hexane-MTBE (1:1 v/v, 5 mL) and re-extracted with hexane (3 mL). The combined organic layers were washed with an aqueous potassium chloride solution (1%, 4 mL), transferred to a new vial, and the KCl mixture was re-extracted with hexane (3 mL). The combined organic layers were evaporated to dryness under a gentle stream of nitrogen. The samples were reconstituted with hexane (1 mL), derivatized with diazomethane in diethyl ether (0.5 mL) for approximately 16 h at 4 °C. All sample extracts underwent sulfur and sulfuric acid clean-up steps[15] prior to gas chromatographic analysis of the concentrated (~100 μL) extracts.

Author Manuscript Author Manuscript Author Manuscript Author Manuscript

Identification of PCB metabolites

GC/TOF-MS analyses were used to identify the hydroxylated PCB metabolites formed in incubations with pHLMs (analyzed as the corresponding methoxylated PCB derivatives). Incubations were performed as described above using the following experimental conditions: 50 μM PCB 91, 90 minute incubation at 37 °C, 0.3 mg/mL microsomal protein, and 1 mM NADPH. Based on metabolism studies with PCB 95,[15] a 90 minute incubation time was expected to yield metabolite levels amenable for GC/TOF-MS analysis. Metabolites were extracted and derivatized as described above, and samples were analyzed on a Waters GCT Premier gas chromatograph (Waters Corporation, Milford, MA, USA) combined with a time-of-flight mass spectrometer in the High Resolution Mass Spectrometry Facility of the University of Iowa (Iowa City, IA, USA). Analytes were separated on a DB-5ms column (30 m length, 250 μm inner diameter, 0.25 μm film thickness; Agilent, Santa Clara, CA, USA). The oven temperature was held at 150 °C for 1 min, then ramped at a rate of 30 °C/min to a final temperature of 240 °C, and held for 15 minutes at 240 °C. The column and temperature program were adopted based on earlier studies separating structurally related OH-PCBs (as methylated derivatives) and modified using authentic standards to allow a rapid GC/TOF-MS analysis.[37, 41] The injector was operated in the splitless mode at a temperature of 280 °C. The helium flow rate was 1.5 mL/min. The source temperature was at 250°C, and a mass range of m/z 50 to 650 was collected. Samples were analyzed with and without continuously introducing heptacosafluorotributylamine as internal standard (or lock mass) to determine the accurate mass of $[M]^+$ and obtain mass spectra of the metabolites. The average relative retention times (RRT) (n=3) of the metabolites, calculated relative to PCB 51 as internal standard, were within 0.5% of the RRT of the respective authentic standard.[42] All experimental accurate mass determinations were within 0.003 Da of the theoretical mass of $[M]^+$, and the isotope patterns of $[M]^+$ matched the theoretical abundance ratios of pentachlorinated biphenyl derivatives with < 20 % error.[42] Gas chromatograms and mass spectra of the metabolites as well as the corresponding authentic standards recorded without heptacosafluorotributylamine are shown in Figure 2 and Figures S3–S10.

Quantification of metabolite levels

To determine the levels of hydroxylated PCB 91 metabolites, sample extracts were analyzed on an Agilent 7890A gas chromatograph with a ^{63}Ni-micro electron capture detector (μECD) and a SPB-1 capillary column (60 m length, 250 μm inner diameter, 0.25 μm film thickness; Supelco, St. Louis, MO, USA) as reported earlier.[43] PCB 204 was added as internal standard (volume corrector) prior to GC analysis. PCB 91 metabolites, as the corresponding methylated derivatives, were quantified based on their respective relative response factors as described previously.[40, 44] The average RRTs of the metabolites, calculated relative to PCB 204, were within 0.5% of the RRT for the respective standard.[42] Formation rates of OH-PCBs are presented adjusted for nmol P450 or microsomal protein content (Tables S3–S6).

Author Manuscript Author Manuscript Author Manuscript Author Manuscript

Enantioselective gas chromatographic analyses

Atropselective analyses of the PCB metabolites were carried out with extracts from the 15 min incubations as in our earlier study.[15] The depletion of PCB 91 atropisomers was also investigated under the following incubation condition: 5 or 50 μM PCB 91, 120 minutes at 37 °C, 0.5 mg/mL protein, and 0.5 mM NADPH) (Table S7).[15] Briefly, extracts were analyzed using an Agilent 6890 gas chromatograph equipped with a ^{63}Ni-μECD detector. PCB 91, 5-91 and 4-91 atropisomers were separated on a ChiralDex B-DM (BDM) capillary column (30 m length, 250 μm inner diameter, 0.12 μm film thickness; Supelco, St Louis, MO, USA). Atropisomers of 3-100 were separated on a ChiralDex G-TA (GTA) capillary column (30 m length, 250 μm inner diameter, 0.12 μm film thickness; Supelco, St Louis, MO, USA).[33, 41] The oven temperature used was modified as follows: 50 °C held for 1 min, ramped at 10 °C/min to 135 °C (140 °C) and held for 750 min (280 min), the temperature was then ramped at 10 °C/min to the final temperature of 200 °C (180 °C) and held for 20 min (40 min) on the BDM (GTA) column. The injector and detector temperatures were both kept at 250 °C. The helium (carrier gas) flow was 3 mL/min. The enantiomeric fraction (EF) was calculated by the drop valley method[45] as EF = Area E_1/(Area E_1 + Area E_2), were Area E_1 and Area E_2 denote the peak area of the first and second eluting atropisomer. To allow a comparison with other studies,[15, 16] all atropisomers discussed below are identified based on their elution order on the columns listed above.

Racemization of PCB 91 and OH-PCB metabolites

The atropisomeric enrichment of PCB 91, 3-100, 5-91 and 4-91 in metabolism studies with HLM was further confirmed by transferring a representative hexane extract from either a 2 hour (5 μM PCB 91; pHLMs) or 15 min incubation (50 μM PCB 91; HLMs from donor H5) into a 2 mL amber ampule. The extract was evaporated to dryness, and the flame-sealed ampule was heated to 300 °C for 2 h as previously described.[33] PCBs with three ortho chlorine substituents have been shown to completely racemize under these conditions.[46] Subsequently, the samples were reconstituted in hexane and analyzed by enantioselective gas chromatography as described above.

Quality assurance/quality control

The response of the μECD was linear ($R^2 \geq 0.999$) for all analytes within the concentration range encountered in this study. The limits of detection (LOD) of the PCB 91 metabolites were calculated from blank buffer samples using the IUPAC method as LOD = mean blanks +k* Standard deviation blanks, (k is the student's t value for a degree of freedom n-1=5 at 99% confidence level).[40, 41] The LODs were 0.14, 0.39, 0.22 and 0.12 ng for 3-100, 5-91, 4-91 and 4,5-91, respectively. The background levels calculated from DMSO blanks were 0.03, 0.25, 0.32 and 0.06 ng/mL for 3-100, 5-91, 4-91 and 4,5-91, respectively. The recoveries of PCB 117 and 4′-159 were 88 ± 8% and 102 ± 10%, respectively. Levels of PCB and its metabolites were not adjusted for recovery to facilitate a comparison with earlier studies.[15, 44] The resolution of the atropisomers of PCB 91, 5-91 and 4-91 on the BDM column was 0.88, 3.60 and 0.68, respectively. The resolution of the atropisomers of 3-100 on the GTA column was 0.86. The EF of the racemic standards of PCB 91, 3-100,

Author Manuscript Author Manuscript Author Manuscript Author Manuscript

5-91 and 4-91 were 0.501 ± 0.001 (n=2), 0.500 ± 0.001 (n=3), 0.498 ± 0.001 (n=3) and 0.47 ± 0.02 (n=3), respectively.

Results and Discussion

Metabolite identification and quantification in pHLMs

The oxidation of PCB 91, a potentially neurotoxic PCB congener[27], by human liver microsomes and the identity of the resulting hydroxylated metabolites has not been investigated to date. GC/TOF-MS analysis revealed the formation of three monohydroxylated and one dihydroxylated metabolite in incubations of racemic PCB 91 with pooled HLMs obtained from 50 mixed gender donors. The identification of these OH-PCB metabolites was confirmed by accurate mass determinations and the chlorine isotope patterns of their molecular ion (analyzed as methylated derivatives). Mass spectra of metabolites identified in PCB 91 incubation with HLM are shown in Figure 2 (for original mass spectra, see Figures S3–S10). Moreover, the fragmentation patterns of the monohydroxylated PCB 91 metabolites were consistent with *meta*- or *para*-methoxylated pentachlorobiphenyl derivatives, with characteristic fragments such as $[M\text{-}CH_3]^+$, $[M\text{-}CH_3\text{-}CO]^+$, $[M\text{-}CH_3\text{-}Cl]^+$, and $[M\text{-}CH_3\text{-}CO\text{-}Cl_2]^+$ (Figure 2). Previous studies reported similar fragmentation pattern for *meta* or *para*, but not *ortho* substituted methylated derivatives of monohydroxylated PCBs or more general derivatives of OH-PCBs, such as the protected trichloroethyl sulfates.[38, 47–49]

Similarly, the mass spectrum of the methylated derivative of the dihydroxylated PCB 91 metabolite showed characteristic fragments, including $[M\text{-}CH_3]^+$, $[M\text{-}CH_3CO]^+$, $[M\text{-}C_2H_6CO]^+$, $[M\text{-}CH_3COCl]^+$, $[M\text{-}C_2H_6COCl]^+$, $[M\text{-}CH_3COCl\text{-}HCl]^+$ and $[M\text{-}C_2H_6(CO)_2Cl]^+$ (Figure 2), as previously observed for the dimethoxy derivative of 4,5-91.[38, 50] The relative retention time and mass spectral information of the metabolites were compared to authentic standard of each analyte for further confirmation of their identity (Figure 1). The PCB 91 structure contains vicinal H substituents in *meta/para* and *ortho/meta* position, sites that are readily metabolized based on published structure-metabolism relationships.[51] We observed hydroxylation in the *meta* and *para* positions of the 2,3,6-trichloro substituted ring, whereas no oxidation was observed in the 2,3,4-chlorophenyl ring. This observation is consistent with earlier observations that lower chlorinated, *ortho* substituted PCBs with a *para* chlorine substituent in one phenyl ring are preferentially oxidized by rat P450 enzymes in the non-*para* substituted ring.[52]

As shown in Figure 3 and Table S2, PCB 91 was mainly oxidized in the *meta* position by both pHLMs and randomly selected individual donor HLMs; with a 1,2-shift product, 3-100, being major metabolite. 5-91 was also formed at high rate, and 4-91 was a minor metabolite. In contrast, 1,2-shift products are minor hydroxylated metabolites formed from PCB 95 and PCB 136 in metabolism studies with HLMs.[15, 16, 34] Although we cannot discount the formation of OH-PCB metabolites of PCB 91 via the direct insertion of oxygen into a C_{Ar}-H bond, the formation of the 1,2-shift product suggests the formation of arene oxide intermediates[53] that subsequently rearrange to the hydroxylated metabolites observed in this study. Because coincubation of PCB 136 with glutathione reduces the formation of 4-136 and 5-136 in metabolism studies with HLMs, the oxidation of PCB 136 by HLMs likely

Author Manuscript Author Manuscript Author Manuscript Author Manuscript

involves arene oxide intermediates as well.[34] Further studies are needed to explain why the 2,3,6-trichlorphenyl ring of structurally related PCB congeners is oxidized with different regioselectivity; assess the formation of other oxidation products, including PCB 91 arene oxides and dihydrodiols;[32, 39, 54, 55] and identify the P450 isoforms involved in their metabolism.[32, 39]

The OH-PCB 91 profiles observed in rodent models, both *in vitro* and *in vivo*, show distinct differences compared to this study with HLMs. Briefly, *in vitro* studies have consistently shown that 5-91 is the major metabolites in incubations with rat liver microsomes,[41] recombinant rat CYP2B1,[55] and precision-cut mouse liver tissue slices.[56] Analogous to the structurally related PCB 51[33] and PCB 52,[32] and several chiral PCBs,[55] oxidation of the *meta* position of PCB 91 by rat CYP2B1 likely occurs *via a* direct insertion of an oxygen atom into aromatic C–H bonds. In contrast, 1,2-shift products are only minor metabolites of PCB 91 and other chiral PCBs in rodent models, both *in vitro* and *in vivo*.[32, 41, 55–58] These findings are not entirely surprising considering the well documented species differences in the metabolism of chiral PCBs.[16, 33, 59, 60]

Inter-individual differences in PCB 91 metabolism by HLMs

Incubations performed with individual donor human liver microsomes provide initial insights into the inter-individual variability of the formation of hydroxylated PCB 91 metabolites (Figure 3). The sum of OH-PCBs (ΣOH-PCBs) formed by the different HLM preparations followed the rank order: H5 > H3 > H2 > H4 ~ pHLM > H1. Levels of ΣOH-PCB were 2.7-fold higher in incubations with HLMs from donors H5 *vs.* donor H1. The levels of ΣOH-PCB 91 in this study were 3.5-fold higher compared to the levels of ΣOH-PCB 95 formed in experiments with the same pHLM preparation, an observation that suggests that PCB 91 may be more rapidly eliminated in humans than PCB 95.[15]

The formation rates of individual PCB 91 metabolite showed pronounced inter-individual differences (Tables S3–S6). For example, the rate of 5-91 formation differed 19-fold for incubations with HLM preparations from donor H1 *vs.* donor H5. The rate of 3-100 and 4-91 formation differed 2.6 and 5.4-fold, respectively, for incubations with HLM preparations from donor H1 *vs.* donor H5. As a consequence, the metabolite profiles formed by individual donor HLM preparations differed for the HLM preparations investigated (Figure 3).

Atropselective analysis

Because PCB 91 is a chiral PCB congener, we explored if PCB 91 is atropselectively metabolized by human P450 enzymes to chiral hydroxylated metabolites. Long-term incubations (5 μM PCB 91) showed an enrichment of the PCB 91 atropisomer eluting first on the BDM column (E_1-PCB 91), with an EF value of 0.53 (Figure 4; panels A1 and A2). EF values for all other incubations were near racemic because the high concentrations on the racemic PCB 91 masked the depletion of a small amount of one atropisomer (Table S7). E_1-PCB 91 was also enriched in Spanish breast milk samples (EF values ranging from 0.53 to 0.65)[14] and in precision cut liver tissue slices from mice.[56] In contrast, the second eluting atropisomer of PCB 91, E_2-PCB 91, was enriched in incubations with rat liver microsomes

Author Manuscript Author Manuscript Author Manuscript Author Manuscript

(EF = 0.43)[41] and recombinant rat CYP2B1 (EF = 0.45).[55] Studies in invertebrates and fish also report an enrichment of E_2-PCB 91.[3] Taken together these studies demonstrate species differences in atropselective metabolism of PCB 91, which is consistent with species differences reported for the metabolism of other PCB congeners.[16, 33]

Atropselective analysis of the hydroxylated PCB metabolites, analyzed as the corresponding methylated derivatives, showed an atropisomeric enrichment of all metabolites investigated (Figure 4; panels B and C). Briefly, the first eluting atropisomer of 3-100 (E_1-3-100; EF range 0.80 to 0.89), second eluting atropisomer of 5-91 (E_2-5-91; EF range 0.37 to 0.48) and first eluting atropisomer of 4-91 (E_1-4-91; EF range 0.71 to 0.90) were enriched in incubation with all microsomal preparations investigated (Figure 5, Table S7). Interestingly, the EF value observed in incubations with individual donor microsomes displayed only relatively small inter-individual differences.[14] Only a limited number of *in* vitro metabolism studies reported the atropselective formation of PCB 91 OH-PCB metabolites. Similar to our study, E_1-3-100 and E_1-5-91 were enriched in incubations with rat liver microsomes,[41] whereas E_2-5-91 was enriched in incubations with rat CYP2B1[55] and in precision cut liver tissue slices from mice.[56] Earlier metabolism studies with PCB 95 and PCB 136 also observed an atropselective formation of OH-PCBs in experiments with HLMs.[15, 16] Taken together, these observations demonstrate species and P450 isoforms dependent differences in enantioselective formation of OH-PCB 91 metabolites.

Two representative extracts containing PCB 91 and its OH-PCB metabolites (as methylated derivatives) were heated at 300 °C for 2 h as previously described to verify that the two peaks observed in the enantioselective analyses are indeed atropisomers of chiral PCB derivatives and not two different PCB metabolites.[33] Subsequent enantioselective analysis revealed essentially a near 1:1 peak ratio for the two atropisomer peaks of 3-100 (EF = 0.87 before *vs.* 0.46 after racemization), 5-91 (EF = 0.43 before *vs.* 0.49 after racemization) and 4-91 (EF = 0.85 before *vs.* 0.51 after racemization) (Figure 4). The EF values of PCB 91 changed from 0.53 to 0.50. Similarly, heating of pure PCB atropisomer above their rotational energy barrier has been shown to result in their rapid racemization.[46]

Environmental and toxicological implications

Chiral PCBs atropselectively affect key biological events implicated in the developmental neurotoxicity of PCBs;[3, 4] however, the processes contributing to the levels of PCB and OH-PCB atropisomers remains poorly characterized in humans. Based on our findings, it seems likely that the enrichment of E_1-PCB 91 in human breast milk and other human samples is due to preferential oxidation of E_2-PCB 91 by human P450 enzymes. Although more studies are needed to support this hypothesis, it is important to emphasize that *in vitro* models in general predict the direction of the atropisomeric enrichment observed in rodent animal models.[3, 4] The present study provides additional evidence that the profiles of metabolites of chiral PCBs formed by human P450 enzymes differ considerably from those observed in rodent species. In addition, the preferential formation of a 1,2-shift product, 3-100, by HLMs revealed a novel, congener specific difference in the metabolism of PCB 91 compared to structurally related PCB congeners, such as PCB 95 and PCB 136, in humans. Together, these finding raise important questions that warrant further attention: 1) Does the

Author Manuscript Author Manuscript Author Manuscript Author Manuscript

atropisomeric enrichment of neurotoxic PCBs play a role in the developmental neurotoxicity of chiral PCBs in humans and can the atropisomeric enrichment be predicted using *in vitro* approaches? 2) Is the developing human brain exposed to different OH-PCB profiles compared to rodent species used in typical developmental neurotoxicity studies? 3) Do chiral OH-PCBs formed by human P450 enzymes atropselectively interact with cellular targets to modulate neurotoxic outcomes?

Supplementary Material

Refer to Web version on PubMed Central for supplementary material.

Acknowledgments

This work was supported by the National Institute of Environmental Health Sciences/National Institutes of Health [grant numbers ES05605, ES013661 and ES027169]. The content of the manuscript is solely the responsibility of the authors and does not necessarily represent the official views of the National Institute of Environmental Health Sciences or the National Institutes of Health. The authors are grateful to Vic Parcell and Lynn Teesch at the University of Iowa High Resolution Mass Spectrometry Facility for help with the GC/TOF-MS analysis.

References

1. Robertson, LW., Hansen, LG. PCBs: recent advances in environmental toxicology and health effects. University Press of Kentucky; 2015.
2. Kania-Korwel I, Lehmler HJ. Toxicokinetics of chiral polychlorinated biphenyls across different species–a review. Environ Sci Pollut Res Int. 2016; 23:2058–2080. [PubMed: 25824003]
3. Lehmler HJ, Harrad SJ, Huhnerfuss H, Kania-Korwel I, Lee CM, Lu Z, Wong CS. Chiral polychlorinated biphenyl transport, metabolism, and distribution: a review. Environ Sci Technol. 2010; 44:2757–2766. [PubMed: 20384371]
4. Kania-Korwel I, Lehmler HJ. Chiral polychlorinated biphenyls: absorption, metabolism and excretion–a review. Environ Sci Pollut Res Int. 2016; 23:2042–2057. [PubMed: 25651810]
5. Mitchell MM, Woods R, Chi LH, Schmidt RJ, Pessah IN, Kostyniak PJ, LaSalle JM. Levels of select PCB and PBDE congeners in human postmortem brain reveal possible environmental involvement in 15q11-q13 duplication autism spectrum disorder. Environ Mol Mutagen. 2012; 53:589–598. [PubMed: 22930557]
6. Wayman GA, Yang D, Bose DD, Lesiak A, Ledoux V, Bruun D, Pessah IN, Lein PJ. PCB-95 promotes dendritic growth via ryanodine receptor-dependent mechanisms. Environ Health Perspect. 2012; 120:997–1002. [PubMed: 22534141]
7. Pessah IN, Cherednichenko G, Lein PJ. Minding the calcium store: Ryanodine receptor activation as a convergent mechanism of PCB toxicity. Pharmacol Ther. 2010; 125:260–285. [PubMed: 19931307]
8. Mariussen E, Fonnum F. Neurochemical targets and behavioral effects of organohalogen compounds: an update. Crit Rev Toxicol. 2006; 36:253–289. [PubMed: 16686424]
9. Kodavanti PR, Curras-Collazo MC. Neuroendocrine actions of organohalogens: thyroid hormones, arginine vasopressin, and neuroplasticity. Front Neuroendocrinol. 2010; 31:479–496. [PubMed: 20609372]
10. Feng W, Zheng J, Robin G, Dong Y, Ichikawa M, Inoue Y, Mori T, Nakano T, Pessah IN. Enantioselectivity of 2,2′,3,5′,6-pentachlorobiphenyl (PCB 95) atropisomers toward ryanodine receptors (RyRs) and their influences on hippocampal neuronal networks. Environ Sci Technol. 2017; 51:14406–14416. [PubMed: 29131945]
11. Dang VD, Walters DM, Lee CM. Transformation of chiral polychlorinated biphenyls (PCBs) in a stream food web. Environ Sci Technol. 2010; 44:2836–2841. [PubMed: 20058914]

Author Manuscript Author Manuscript Author Manuscript Author Manuscript

12. Wong CS, Garrison AW, Smith PD, Foreman WT. Enantiomeric composition of chiral polychlorinated biphenyl atropisomers in aquatic and riparian biota. Environ Sci Technol. 2001; 35:2448–2454. [PubMed: 11432547]
13. Wong CS, Mabury SA, Whittle DM, Backus SM, Teixeira C, DeVault DS, Bronte CR, Muir DC. Organochlorine compounds in Lake Superior: chiral polychlorinated biphenyls and biotransformation in the aquatic food web. Environ Sci Technol. 2004; 38:84–92. [PubMed: 14740721]
14. Bordajandi LR, Abad E, Gonzalez MJ. Occurrence of PCBs, PCDD/Fs, PBDEs and DDTs in Spanish breast milk: enantiomeric fraction of chiral PCBs. Chemosphere. 2008; 70:567–575. [PubMed: 17727913]
15. Uwimana E, Li X, Lehmler HJ. 2,2′,3,5′,6-Pentachlorobiphenyl (PCB 95) is atropselectively metabolized to para-hydroxylated metabolites by human liver microsomes. Chem Res Toxicol. 2016; 29:2108–2110. [PubMed: 27989147]
16. Wu X, Kammerer A, Lehmler HJ. Microsomal oxidation of 2,2′,3,3′,6,6′-hexachlorobiphenyl (PCB 136) results in species-dependent chiral signatures of the hydroxylated metabolites. Environ Sci Technol. 2014; 48:2436–2444. [PubMed: 24467194]
17. Tehrani R, Van Aken B. Hydroxylated polychlorinated biphenyls in the environment: sources, fate, and toxicities. Environ Sci Pollut Res Int. 2014; 21:6334–6345. [PubMed: 23636595]
18. Grimm FA, Hu D, Kania-Korwel I, Lehmler HJ, Ludewig G, Hornbuckle KC, Duffel MW, Bergman A, Robertson LW. Metabolism and metabolites of polychlorinated biphenyls. Crit Rev Toxicol. 2015; 45:245–272. [PubMed: 25629923]
19. Kania-Korwel I, Lukasiewicz T, Barnhart CD, Stamou M, Chung H, Kelly KM, Bandiera S, Lein PJ, Lehmler HJ. Editor's highlight: Congener-specific disposition of chiral polychlorinated biphenyls in lactating mice and their offspring: implications for PCB developmental neurotoxicity. Toxicol Sci. 2017; 158:101–115. [PubMed: 28431184]
20. Bergman A, Klasson-Wehler E, Kuroki H. Selective retention of hydroxylated PCB metabolites in blood. Environ Health Perspect. 1994; 102:464–469. [PubMed: 8593850]
21. Quinete N, Esser A, Kraus T, Schettgen T. PCB 28 metabolites elimination kinetics in human plasma on a real case scenario: Study of hydroxylated polychlorinated biphenyl (OH-PCB) metabolites of PCB 28 in a highly exposed German Cohort. Toxicol Lett. 2017; 276:100–107. [PubMed: 28552772]
22. Meerts IA, Assink Y, Cenijn PH, Van Den Berg JH, Weijers BM, Bergman A, Koeman JH, Brouwer A. Placental transfer of a hydroxylated polychlorinated biphenyl and effects on fetal and maternal thyroid hormone homeostasis in the rat. Toxicol Sci. 2002; 68:361–371. [PubMed: 12151632]
23. Lucier GW, McDaniel OS, Schiller CM, Matthews HB. Structural requirements for the accumulation of chlorinated biphenyl metabolites in the fetal rat intestine. Drug Metab Dispos. 1978; 6:584–590. [PubMed: 30609]
24. Park HY, Park JS, Sovcikova E, Kocan A, Linderholm L, Bergman A, Trnovec T, Hertz-Picciotto I. Exposure to hydroxylated polychlorinated biphenyls (OH-PCBs) in the prenatal period and subsequent neurodevelopment in eastern Slovakia. Environ Health Perspect. 2009; 117:1600–1606. [PubMed: 20019912]
25. Berghuis SA, Soechitram SD, Hitzert MM, Sauer PJ, Bos AF. Prenatal exposure to polychlorinated biphenyls and their hydroxylated metabolites is associated with motor development of three-month-old infants. Neurotoxicology. 2013; 38:124–130. [PubMed: 23895877]
26. Berghuis SA, Soechitram SD, Sauer PJ, Bos AF. Prenatal exposure to polychlorinated biphenyls and their hydroxylated metabolites is associated with neurological functioning in 3-month-old infants. Toxicol Sci. 2014; 142:455–462. [PubMed: 25246668]
27. Niknam Y, Feng W, Cherednichenko G, Dong Y, Joshi SN, Vyas SM, Lehmler HJ, Pessah IN. Structure-activity relationship of selected meta- and para-hydroxylated non-dioxin like polychlorinated biphenyls: from single RyR1 channels to muscle dysfunction. Toxicol Sci. 2013; 136:500–513. [PubMed: 24014653]
28. Pessah IN, Hansen LG, Albertson TE, Garner CE, Ta TA, Do Z, Kim KH, Wong PW. Structure-activity relationship for noncoplanar polychlorinated biphenyl congeners toward the ryanodine

Author Manuscript Author Manuscript Author Manuscript Author Manuscript

receptor-Ca^{2+} channel complex type 1 (RyR1). Chem Res Toxicol. 2006; 19:92–101. [PubMed: 16411661]

29. Dhakal K, Gadupudi GS, Lehmler HJ, Ludewig G, Duffel MW, Robertson LW. Sources and toxicities of phenolic polychlorinated biphenyls (OH-PCBs). Environ Sci Pollut Res Int. 2017; doi: 10.1007/s11356-017-9694-x
30. Forgue ST, Preston BD, Hargraves WA, Reich IL, Allen JR. Direct evidence that an arene oxide is a metabolic intermediate of 2,2′,5,5′-tetrachlorobiphenyl. Biochem Biophys Res Commun. 1979; 91:475–483. [PubMed: 42397]
31. Forgue ST, Allen JR. Identification of an arene oxide metabolite of 2,2′,5-5′-tetrachlorobiphenyl by gas chromatography-mass spectroscopy. Chem Biol Interact. 1982; 40:233–245. [PubMed: 6805966]
32. Preston BD, Miller JA, Miller EC. Non-arene oxide aromatic ring hydroxylation of 2,2′,5,5′-tetrachlorobiphenyl as the major metabolic pathway catalyzed by phenobarbital-induced rat liver microsomes. J Biol Chem. 1983; 258:8304–8311. [PubMed: 6408087]
33. Uwimana E, Maiers A, Li X, Lehmler HJ. Microsomal metabolism of prochiral polychlorinated biphenyls results in the enantioselective formation of chiral metabolites. Environ Sci Technol. 2017; 51:1820–1829. [PubMed: 28038482]
34. Schnellmann RG, Putnam CW, Sipes IG. Metabolism of 2,2′,3,3′,6,6′-hexachlorobiphenyl and 2,2′,4,4′,5,5′-hexachlorobiphenyl by human hepatic microsomes. Biochem Pharmacol. 1983; 32:3233–3239. [PubMed: 6416258]
35. McGraw JE Sr, Waller DP. Specific human CYP 450 isoform metabolism of a pentachlorobiphenyl (PCB-IUPAC# 101). Biochem Biophys Res Commun. 2006; 344:129–133. [PubMed: 16616008]
36. DeCaprio AP, Johnson GW, Tarbell AM, Carpenter DO, Chiarenzelli JR, Morse GS, Santiago-Rivera AL, Schymura MJ, Akwesasne Task Force on the, E. Polychlorinated biphenyl (PCB) exposure assessment by multivariate statistical analysis of serum congener profiles in an adult Native American population. Environ Res. 2005; 98:284–302. [PubMed: 15910784]
37. Kania-Korwel I, Vyas SM, Song Y, Lehmler HJ. Gas chromatographic separation of methoxylated polychlorinated biphenyl atropisomers. J Chromatogr A. 2008; 1207:146–154. [PubMed: 18760792]
38. Joshi SN, Vyas SM, Duffel MW, Parkin S, Lehmler HJ. Synthesis of sterically hindered polychlorinated biphenyl derivatives. Synthesis. 2011; 7:1045–1054. [PubMed: 21516177]
39. McLean MR, Bauer U, Amaro AR, Robertson LW. Identification of catechol and hydroquinone metabolites of 4-monochlorobiphenyl. Chem Res Toxicol. 1996; 9:158–164. [PubMed: 8924585]
40. Wu X, Pramanik A, Duffel MW, Hrycay EG, Bandiera SM, Lehmler HJ, Kania-Korwel I. 2,2′,3,3′,6,6′-Hexachlorobiphenyl (PCB 136) is enantioselectively oxidized to hydroxylated metabolites by rat liver microsomes. Chem Res Toxicol. 2011; 24:2249–2257. [PubMed: 22026639]
41. Kania-Korwel I, Duffel MW, Lehmler HJ. Gas chromatographic analysis with chiral cyclodextrin phases reveals the enantioselective formation of hydroxylated polychlorinated biphenyls by rat liver microsomes. Environ Sci Technol. 2011; 45:9590–9596. [PubMed: 21966948]
42. Commission E. Commission decision EC 2002/657 of 12 August 2002 implementing Council Directive 96/23/EC concerning the performance of analytical methods and the interpretation of results. Off J Eur Communities: Legis. 2002; 221
43. Wu X, Kania-Korwel I, Chen H, Stamou M, Dammanahalli KJ, Duffel M, Lein PJ, Lehmler HJ. Metabolism of 2,2′,3,3′,6,6′-hexachlorobiphenyl (PCB 136) atropisomers in tissue slices from phenobarbital or dexamethasone-induced rats is sex-dependent. Xenobiotica. 2013; 43:933–947. [PubMed: 23581876]
44. Wu X, Lehmler HJ. Effects of thiol antioxidants on the atropselective oxidation of 2,2′,3,3′,6,6′-hexachlorobiphenyl (PCB 136) by rat liver microsomes. Environ Sci Pollut Res Int. 2016; 23:2081–2088. [PubMed: 26155892]
45. Asher BJ, D'Agostino LA, Way JD, Wong CS, Harynuk JJ. Comparison of peak integration methods for the determination of enantiomeric fraction in environmental samples. Chemosphere. 2009; 75:1042–1048. [PubMed: 19215960]

Author Manuscript Author Manuscript Author Manuscript Author Manuscript

46. Harju MT, Haglund P. Determination of the rotational energy barriers of atropisomeric polychlorinated biphenyls. Fresen J Anal Chem. 1999; 364:219–223.
47. Li X, Robertson LW, Lehmler HJ. Electron ionization mass spectral fragmentation study of sulfation derivatives of polychlorinated biphenyls. Chem Cent J. 2009; 3:5. [PubMed: 19272150]
48. Bergman A, Klasson WE, Kuroki H, Nilsson A. Synthesis and mass-spectrometry of some methoxylated PCB. Chemosphere. 1995; 30:1921–1938.
49. Jansson B, Sundström G. Mass spectrometry of the methyl ethers of isomeric hydroxychlorobiphenyls—potential metabolites of chlorobiphenyls. Biol Mass Spectrom. 1974; 1:386–392.
50. Haraguchi K, Kato Y, Koga N, Degawa M. Metabolism of polychlorinated biphenyls by Gunn rats: identification and serum retention of catechol metabolites. Chem Res Toxicol. 2004; 17:1684–1691. [PubMed: 15606145]
51. Blanch GP, Glausch A, Schurig V. Determination of the enantiomeric ratios of chiral PCB 95 and 149 in human milk samples by multidimensional gas chromatography with ECD and MS(SIM) detection. Eur Food Res Technol. 1999; 209:294–296.
52. Kennedy MW, Carpentier NK, Dymerski PP, Kaminsky LS. Metabolism of dichlorobiphenyls by hepatic microsomal cytochrome P-450. Biochem Pharmacol. 1981; 30:577–588. [PubMed: 6791661]
53. Guroff G, Daly JW, Jerina DM, Renson J, Witkop B, Udenfriend S. Hydroxylation-induced migration: the NIH shift. Recent experiments reveal an unexpected and general result of enzymatic hydroxylation of aromatic compounds. Science. 1967; 157:1524–1530. [PubMed: 6038165]
54. Waller SC, He YA, Harlow GR, He YQ, Mash EA, Halpert JR. 2,2′,3,3′,6,6′-hexachlorobiphenyl hydroxylation by active site mutants of cytochrome P450 2B1 and 2B11. Chem Res Toxicol. 1999; 12:690–699. [PubMed: 10458702]
55. Lu Z, Kania-Korwel I, Lehmler H-J, Wong CS. Stereoselective formation of mono- and di-hydroxylated polychlorinated biphenyls by rat cytochrome P450 2B1. Environ Sci Technol. 2013; 47:12184–12192. [PubMed: 24060104]
56. Wu X, Duffel M, Lehmler HJ. Oxidation of polychlorinated biphenyls by liver tissue slices from phenobarbital-pretreated mice is congener-specific and atropselective. Chem Res Toxicol. 2013; 26:1642–1651. [PubMed: 24107130]
57. Kato S, McKinney JD, Matthews HB. Metabolism of symmetrical hexachlorobiphenyl isomers in the rat. Toxicol Appl Pharmacol. 1980; 53:389–398. [PubMed: 6770495]
58. Van Miller JP, Hsu IC, Allen JR. Distribution and metabolism of ^{3}H-2,5,2′,5′-tetrachlorobiphenyl in rats. Proc Soc Exp Biol Med. 1975; 148:682–687. [PubMed: 805431]
59. Hsu IC, van Miller JP, Seymour JL, Allen JR. Urinary metabolites of 2, 5, 2′, 5′-tetrachlorobiphenyl in the nonhuman primate. Proc Soc Exp Biol Med. 1975; 150:185–188. [PubMed: 810809]
60. Hsu IC, Van Miller JP, Allen JR. Metabolic fate of ^{3}H 2,5,2′,5′-tetrachlorobiphenyl in infant nonhuman primates. Bull Environ Contam Toxicol. 1975; 14:233–240. [PubMed: 809075]

Author Manuscript Author Manuscript Author Manuscript Author Manuscript

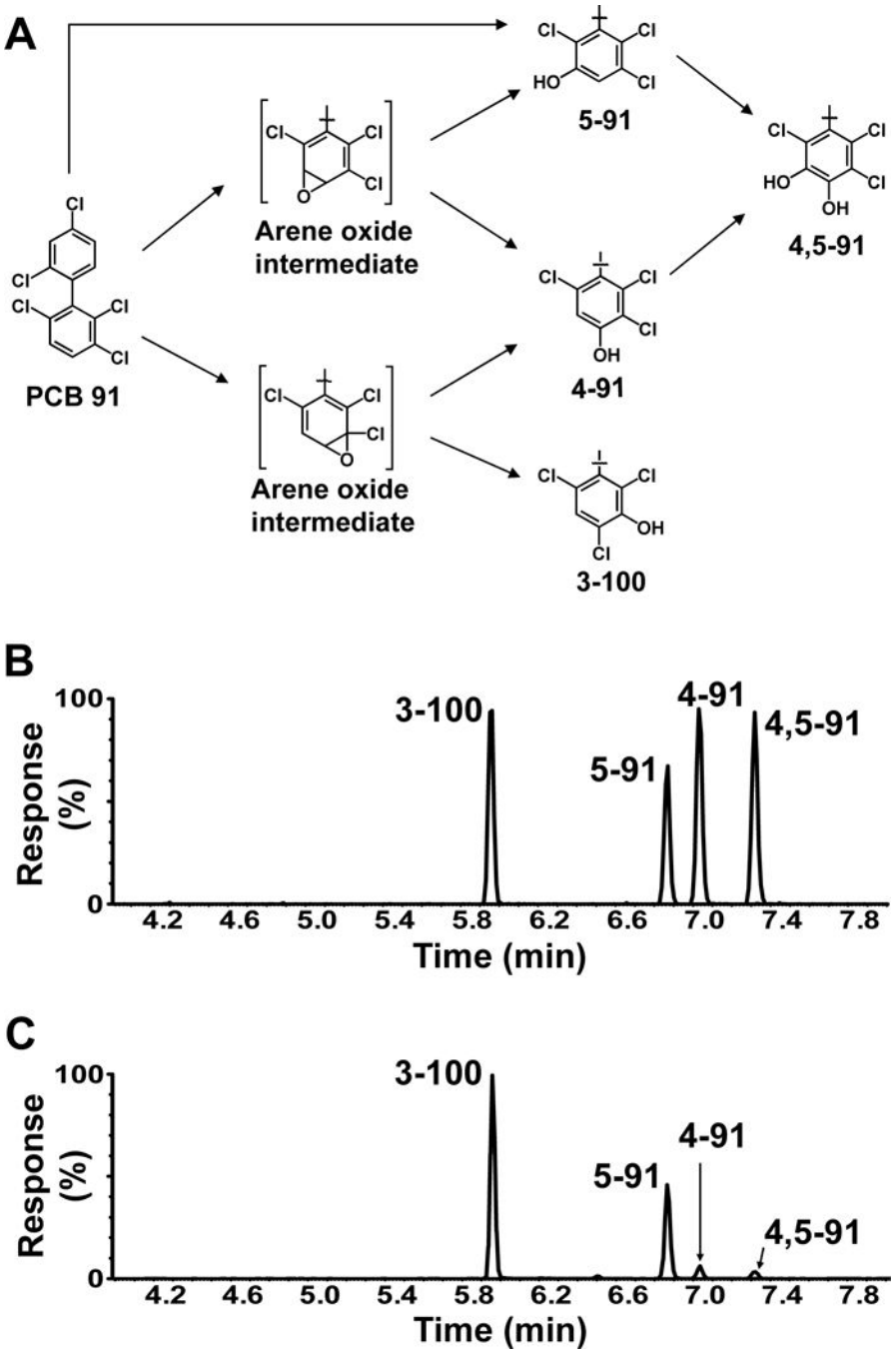

Figure 1. PCB 91 biotransformation by pHLMs reveals the formation of three monohydroxylated (*m/z* 355.9) and one dihydroxylated (*m/z* 385.9) metabolites (analyzed as methylated derivatives)

(A) Simplified metabolism scheme showing the chemical structure and abbreviations of racemic PCB 91 metabolites identified. Representative GC-TOF chromatograms of (B) PCB 91 metabolite standards and (C) an extract from an incubation with pHLMs (50 μM PCB 91, 90 minutes, 37 °C, 0.3 mg/mL protein, and 1 mM NADPH). See Figure 2 for mass spectra of metabolites in incubation extracts. The metabolites were identified based on their

retention times relative to the corresponding authentic standard and their *m/z.* See Experimental section for GC-MS analysis conditions.

Author Manuscript Author Manuscript Author Manuscript Author Manuscript

Author Manuscript Author Manuscript Author Manuscript Author Manuscript

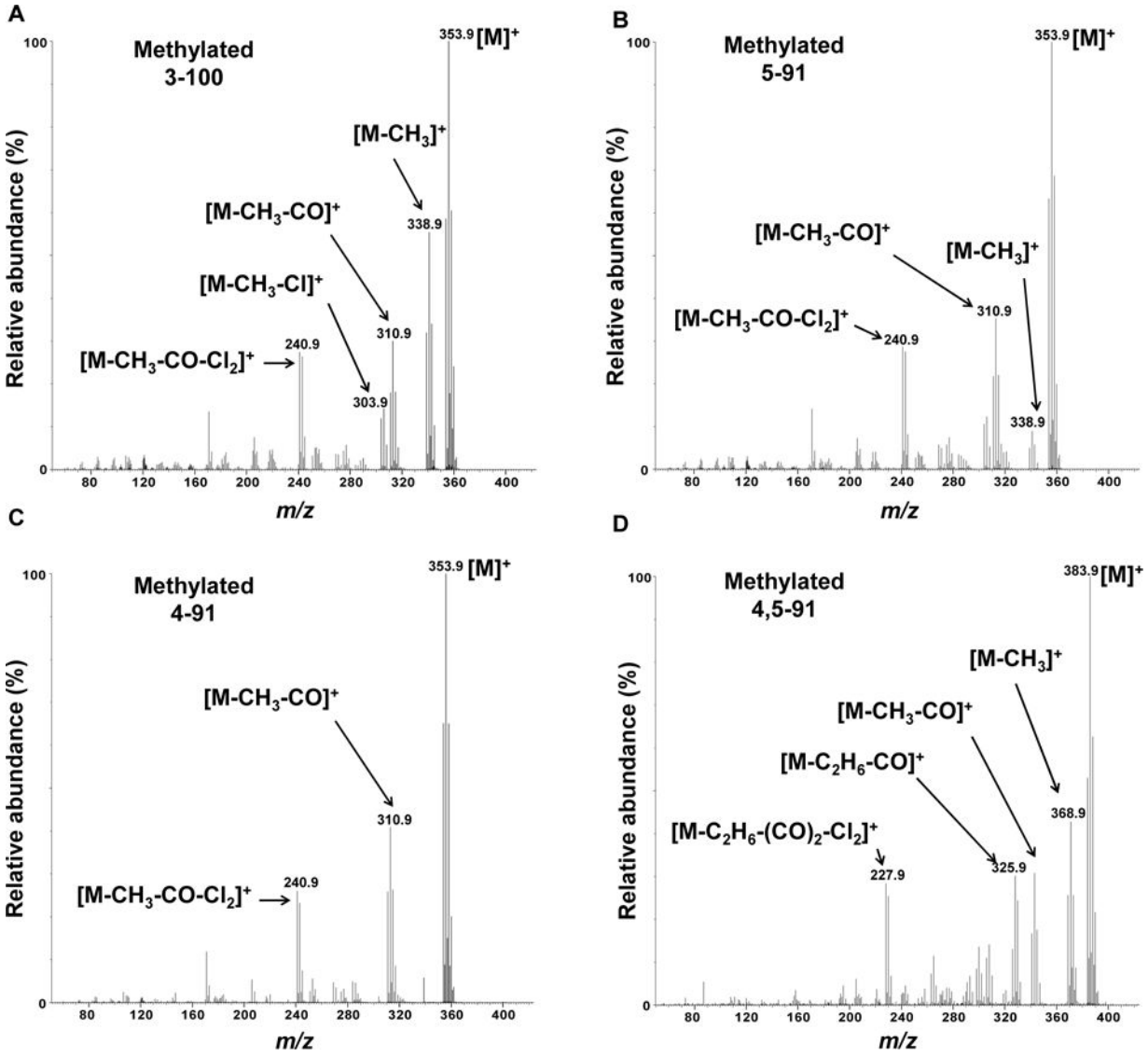

Figure 2. Mass spectra showing typical fragmentation patterns of hydroxylated pentachlorobiphenyls (as methylated derivatives) support the formation of (A) 3-100; (B) 5-91; (C) 4-91; and (D) 4,5-91 in incubations of racemic PCB 91 with pHLM

See Figure 1C for the corresponding gas chromatogram.

Author Manuscript Author Manuscript Author Manuscript Author Manuscript

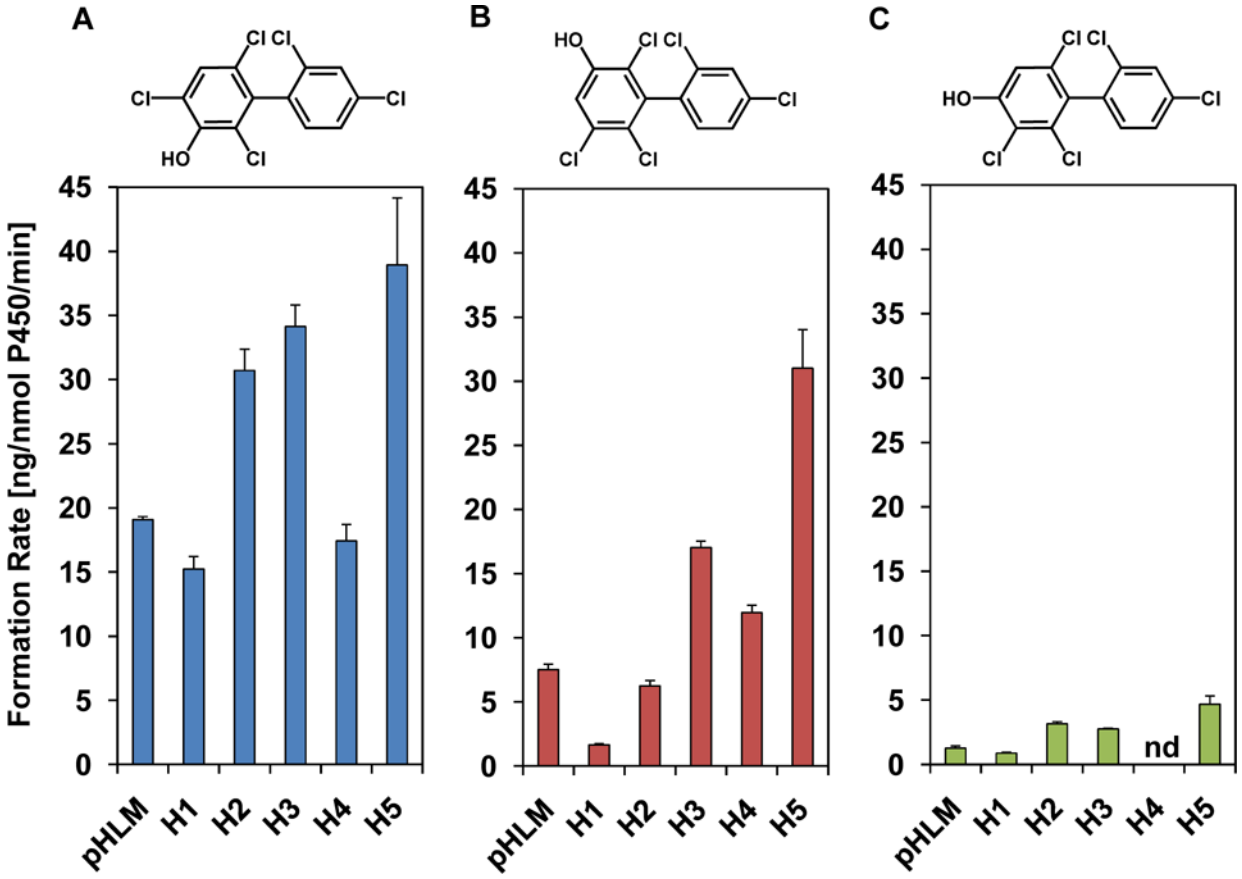

Figure 3. Comparison of the OH-PCB formation rates reveals inter-individual differences in the metabolism of racemic PCB 91 by different HLM preparations, with (A) the 1,2-shift metabolite, 3-100, and (B) 5-91 being major metabolites, and (C) 4-91 being a minor metabolite

Incubations were carried out with 50 μM racemic PCB 91, 0.1 mg/mL microsomal protein and 1 mM NADPH for 5 min at 37 °C.[15] Extracts from the microsomal incubations were derivatized with diazomethane and analyzed by GC-μECD; see the Experimental Section for additional details. Data are presented as mean ± standard deviation, n = 3.

Author Manuscript Author Manuscript Author Manuscript Author Manuscript

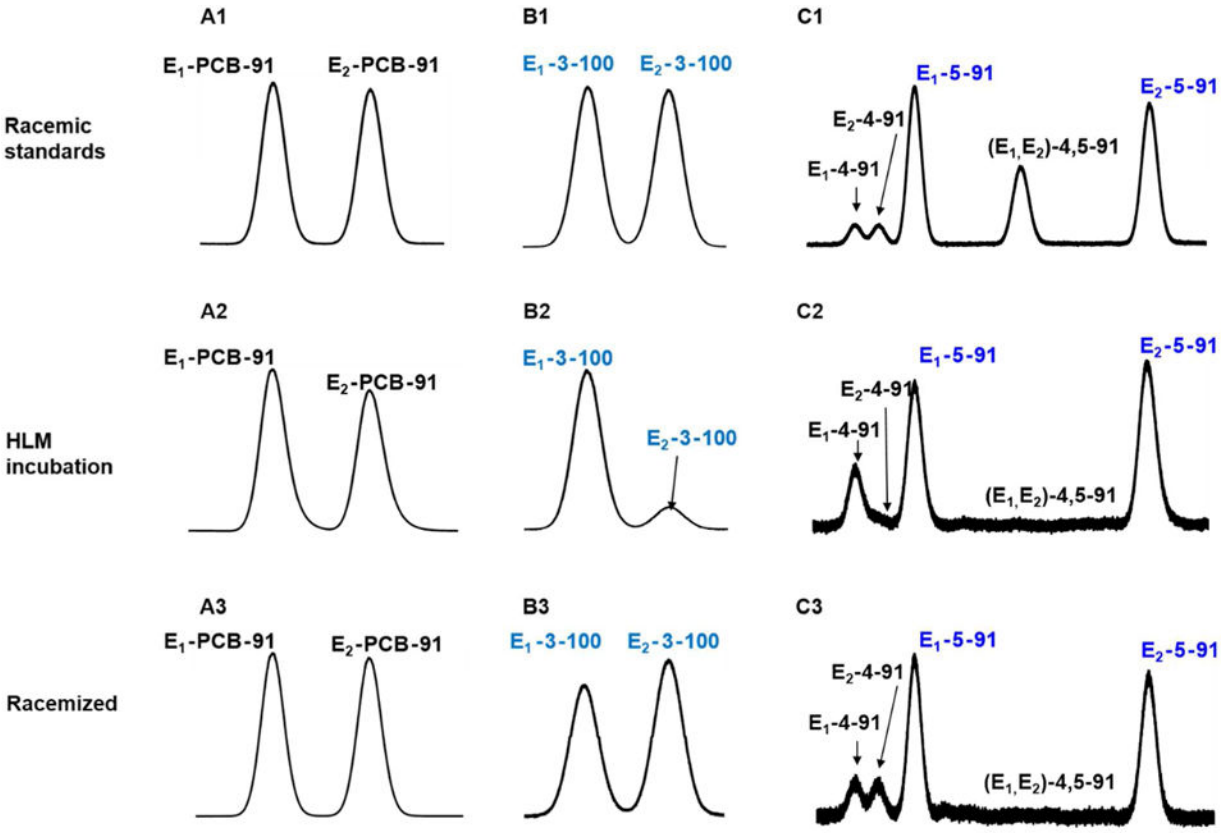

Figure 4. Atropselective analysis revealed the atropselective metabolism of racemic PCB 91 to chiral OH-PCBs 3-100, 5-91 and 4-91

Representative gas chromatograms comparing racemic standards (top panels) to PCB 91, 3-100, 5-91 and 4,-91 extracted from incubations of racemic PCB 91 with human liver microsomes (bottom panels) and the corresponding racemized incubation extract (bottom panels). The chromatograms demonstrate depletion of E_2-PCB 91 **(A1 *vs.* A2)** and enantioselective formation of E_1-3-100 **(B1 *vs.* B2)**, E_1-4-91 **(C1 *vs.* C2)** and E_2-5-91 **(C1 *vs.* C2)**. To verify that the two peaks observed in the enantioselective analyses are indeed atropisomers of chiral PCB derivatives and not two different PCB metabolites, extracts were racemized at 300 °C and reanalyzed by enantioselective gas chromatography (panels **A3**, **B3** and **C3**). To assess the atropselective depletion of PCB 91, incubations were carried out with 5 μM PCB 91, 0.5 mg/mL microsomal protein (only pooled human liver microsomes were used) and 0.5 mM NADPH for 2 h at 37 °C. To study the atropselective formation of the PCB 91 metabolites, incubations were carried out with 50 μM racemic PCB 91, 0.1 mg/mL microsomal protein and 1 mM NADPH for 15 min at 37 °C (donor H5 shown here; see Figure 5 for results from incubations using other human liver microsome preparations).[15] Metabolites were analyzed as the corresponding methylated derivatives after derivatization with diazomethane. Atropselective analyses of PCB 91, 5-91 and 4-91 were carried out with a ChiralDex B-DM capillary column at 135 °C.[41] Atropselective analyses of 3-100 were performed with a ChiralDex GTA capillary column at 140 °C.[41]

Author Manuscript Author Manuscript Author Manuscript Author Manuscript

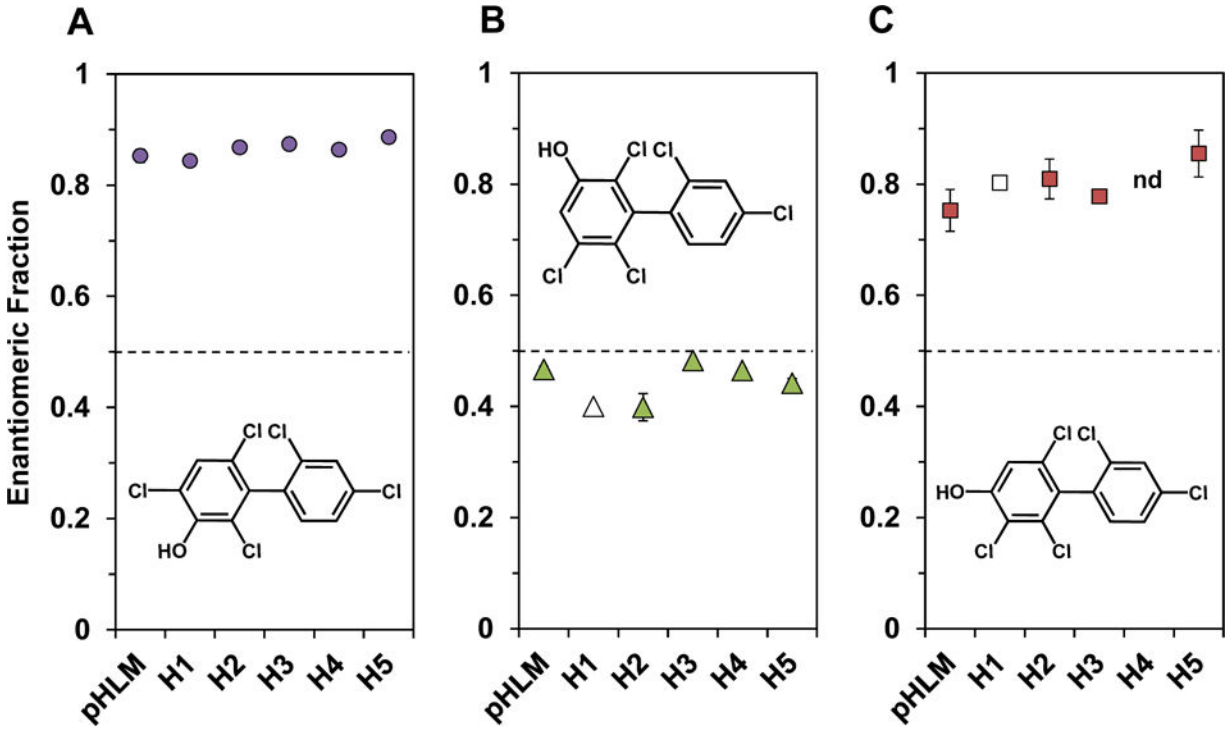

Figure 5. Enantiomeric fractions (EFs) of 3-100 and 4-91 and 5-91 reveal only small interindividual differences in the enantioselective formation of OH-PCB 91 metabolites

Microsomal incubations were carried out with 50 μM racemic PCB 91, 0.1 mg/mL microsomal protein, 1 mM NADPH for 15 min at 37 °C.[15] Metabolites were analyzed as the corresponding methylated derivatives after derivatization with diazomethane. Atropselective analyses of 5-91 and 4-91 were carried out with a ChiralDex B-DM capillary column at 135 °C.[41] Atropselective analyses of 3-100 were performed with a ChiralDex GTA capillary column at 140 °C.[41] Data are presented as mean ± standard deviation, n = 3. Open symbols indicate n = 1. nd = not detected. The dotted line indicates the EF values of the racemic standards.